Research article

Computational model for detection of abnormal brain connections in children with autism

Elham Askari[1], Seyed Kamaledin Setarehdan[2,*], Ali Sheikhani[3], Mohammad Reza Mohammadi[4], Mohammad Teshnehlab[5]

[1] Department of Computer Engineering, Science and Research Branch, Islamic Azad University, Tehran, Iran
[2] Control and Intelligent Processing Center of Excellence, School of Electrical and Computer Engineering, College of Engineering, University of Tehran, Tehran, Iran
[3] Department of Biomedical Engineering, Science and Research Branch, Islamic Azad University, Tehran, Iran
[4] Psychiatry and Psychology Research Center, Roozbeh Hospital, Tehran University of Medical Sciences, Tehran, Iran
[5] Department of Control Engineering, K.N. Toosi University of Technology, Tehran, Iran

*Correspondence: ksetareh@ut.ac.ir (Seyed Kamaledin Setarehdan)

https://doi.org/10.31083/JIN-180075

Abstract

In neuropsychological disorders significant abnormalities in brain connectivity are observed in some regions. A novel model demonstrates connectivity between different brain regions in children with autism. Wavelet decomposition is used to extract features such as relative energy and entropy from electroencephalograph signals. These features are used as input to a 3D-cellular neural network model that indicates brain connectivity. Results show significant differences and abnormalities in the left hemisphere, ($p < 0.05$) at electrodes AF3, F3, P7, T7, and O1 in the alpha band, AF3, F7, T7, and O1 in the beta band, and T7 and P7 in the gamma band for children with autism when compared with non-autistic controls. Abnormalities in the connectivity of frontal and parietal lobes and the relations of neighboring regions for all three bands (particularly the gamma band) were detected for autistic children. Evaluation demonstrated the alpha frequency band had the best level of distinction (96.6%) based on the values obtained from a cellular neural network that employed support vector machine methods.

Keywords

Autism; electroencephalography; 3D-cellular neural network; wavelet transform; Emotiv epoch

Submitted: May 13, 2017; **Accepted:** November 16, 2017

1. Introduction

The brain is the most important and complex human organ. Behavior, feelings, perceptions, and normal social interactions are possible through a healthy brain [1]. Some studies conducted on individual brain organization, suggest certain patterns and connections in different regions of the brain in various human conditions and also show abnormalities in brain organization and connectivity of individuals with neuropsychological diseases [2]. Johansen-Berg *et al.* [3] asserted that by looking at the physical connections between regions, known as structural connectivity, or by looking at similarities of the temporal characteristics of brain activity in different regions, referred to as functional connectivity, brain connectivity can be examined. According to these studies there is evidence for both types of connectivity and that these measures provide means by which such regions communicate with each other. Moreover, it has been reported that during active processes such as perception and cognitive processing, brain regions demonstrate temporal correlations of activation patterns. Buckner *et al.* [4] mentioned that brain regions demonstrate temporal correlations of activation patterns during rest as well.

Task related functional connectivity provides evidence of which networks of brain regions are recruited to process and integrate information and to respond adequately to task demands [5]. In two other studies Assaf *et al.* [5] and Weng *et al.* [6] reported that resting-state functional connectivity was investigated without external stimulation. To do so, people were typically trained to close their eyes and think about nothing for about 5–10 min [6, 7]. It was demonstrated that functional connectivity between the precuneus and medial prefrontal cortex, both default mode network core areas, and other default mode sub-networks areas decreased.

Autism is one disease that directly affects human brain function and connectivity [8]. The term "autism" was introduced by Kanner [9]. Autism is a neurological disorder with psychological symptoms, usually appears in the first three years of life, and is associated with disturbances in social relations and personal perception. Statistics show the annual prevalence of the disease is 6 per 1000 people [10].

Electroencephalography (EEG) is an electrophysiological monitoring method used to evaluate several types of brain disorder. In subjects with autism it reports abnormal brain activities and suggests there is an underlying structural disorder [11]. EEG can be used for diagnostic purposes and conclusions can be drawn from the shape and power of the signal in a particular frequency band. EEG and magnetoencephalography are also used to localize neural activity [12]. EEG provides reliable information about some of the activities and interactions of the brain [13]. Information and features can be extracted through accurate recording and computer analysis of these signals. Furthermore, some brain and mental disorders can be diagnosed through studying such processes.

Many investigators have studied the EEGs and analyzed the signals of autistic subjects [14–16]. Sheikhani *et al.* [15] conducted a study of EEG signals based on Lempel–Ziv frequency methods (LZ) and the short-time Fourier transform (STFT). After evaluating results,

non-autistic and autistic subjects could be distinguished with 81% accuracy. In another study, independent component analysis was also employed and the possibility of extracting independent sources of EEG signals and correlations between different brain autistic regions was investigated [17]. It was determined that the correlation in the left hemisphere (including F3, C3, and P3 channels) for autistic subjects is lower than in these regions for non-autistic subjects [15–17]. Since the left hemisphere is responsible for speech-related activities, the lack of engagement in this region in autistics may be one of the reasons for the problems of these people [15]. According to studies conducted by Von Stein [18] and Sheikhani [10], the average of the gamma frequency band in some components of the left hemisphere for autistic subjects is higher than found for non-autistic subjects and is lower for the theta band. With regard to the fast Fourier transform and componential correlation analysis, some differences have been observed in the left hemisphere of autistics. After statistical analysis, an attempt was made to draw brain organization and a binding map [17]. In another study, Sheikhani [10] used EEG spectrogram analysis for autistic and control non-autistic subjects. It was claimed that the best differentiation between them was obtained from the alpha band during a relaxed eye-open condition [10]. Orekhova [19] studied high-frequencies of the power spectrum of autistic groups across the age range of 3–8 years and showed that high gamma-band activity was determined by the spatial distance of recording electrodes from sources that generated muscle artifacts. Dumas *et al.* [20] examined the whole brain and a hypothesis that there is functional dissociation of μ and α responses to the observation of human actions in autistic spectrum disorder according to band widths. Source reconstructions showed this impact was related to a joint μ-suppression deficit over the occipito-parietal regions and that it was also related to increase over the frontal regions [20].

Just *et al.* [21] and Vissers *et al.* [5, 21] discussed the abnormalities in brain connectivity of children with autism. In the absence of a connection theory, the lack of which was mentioned by Just, functional magnetic resonance imaging was employed to investigate both the inter-cellular connections of anterior and posterior cortex and the problem of reduced interaction between the anterior regions and parietal lobe in people with autism [21]. Just noted that many of the previous models were neural network or connectionist models that carefully examined the possibility that autism is characterized by abnormalities at the level of individual connectionist units and weights in a neural network. For instance, Cohen showed that poor generalization in autism is caused by inadequate numbers of hidden units [22]. McClelland *et al.* [23], Gustafsson *et al.* [24], and OLaughlin and Thagard [25], proposed it was a consequence, respectively, of excessive conjunction coding and excessive inhibition, under-aroused depression in the amygdala, hypervigilant learning in temporal and prefrontal cortices, and the failure of adaptive timing in hippocampal and cerebellar regions. Brock *et al.* [26] ascribed weak central coherence to an impairment of temporal binding between local networks, whereas temporal binding within local networks was supposed to be intact or possibly even enhanced.

Niederhoefer *et al.* [27, 28] reviewed different approaches to the analysis of EEG signals based on cellular neural networks. They studied several methods of EEG analysis based on multi-layer convolutional neural networks (CNN) for seizure and discussed approximation of the correlation dimension, prediction of EEG-signals, and an EEG pattern detection algorithm. Subsequently, they investigated prediction algorithms and the calculation of synchronization measures for EEG by multi-layer CNN in epilepsy disorder [29]. Muller *et al.* [30] proposeda new architecture for the hardware emulation of discrete-time cellular neural networks (DT-CNN) suited to EEG signal processing in epilepsy. Results of the proposed CNN architecture showed the importance of high computational accuracy for EEG signal processing prediction that was not possible with analogue VLSI circuits.

Very few models have been based on specific experimental data [21]. Balkenius [31] attempted to present a model for compensating attention-switching deficits during cognition. Grossberg and Seidman [32] proposed a complex connectionist model for autism. The model employs an imbalance of parameters among three component subsystems. Only one previous computational model has provided a general account of autism [21]. Noriega [33, 34] used a self-organizing map neural network to show perceptual abnormalities in the autistic brain. It was claimed that weak central coherence causes disruption to key regions of the brain and imbalance in excitatory-inhibitory networks. Papageorgiou *et al.* [35] proposed a model to identify autism based on a fuzzy cognitive map (FCM) that was trained by a nonlinear Hebbian learning algorithm (NHL). Results demonstrated that the proposed FCM ensemble algorithm was better than the NHL based approach alone with respect to the accuracy of FCM learning.

Previous studies have confirmed the differences between EEG signals and the region connections of autistic and non-autistic groups. In the aforementioned methods for separating two groups, statistical methods were used to distinguish them by EEG signals, without presenting a unique model of the brain function. Furthermore, those methods, weren't able to extract intra-region connections from EEG signals. However, by employing the 3D-cellular neural network (two-layer CNN) model presented here and including the proper EEG features, based on an intelligent system, it is possible to show the connectivity of the various brain regions and also distinguish autistic and non-autistic subjects. This model considers the volume conduction of the human brain. In the model all regions connect with their adjacent and non-adjacent regions and it identifies the intra- and inter-region connectivity.

2. Materials and methods

This method includes three basic phases: signal recording, signal analysis, and brain modeling.

2.1. Subjects

Recorded signals were collected from 100 autistic children (50 males and 50 females) aged between 5 and 12 years and 100 non-autistic children (50 males and 50 females) with the same age range. The average age of the subjects with autism and the non-autistic controls was 9.7 $\pm$ 2.3 (mean $\pm$ standard deviation) and 9.3 $\pm$ 1.9, respectively. A *t*-test on age showed no significant difference between the two groups (p = 0.532). Diagnosis was performed by two expert child and adolescent psychiatrists based on the DSM-IV-TR (Diagnostic and statistical manual of mental disorder [36]). All subjects with autistic spectrum disorder were medication-free for at least two weeks prior to EEG recording. The non-autistic group was selected from healthy school children with no history of neurological disorder or prescribed medicine. The subjects participated in this study with both parental and self consent. All subjects had a full-scale intelligence quotient greater than 85 [37].

2.2. *EEG recording*

Signal recording was conducted when subjects were awake with open eyes and calmly seated on a chair. Signals were recorded from each subject for 18 minutes. The recording was conducted at the research center of psychology and psychiatry, Roozbeh Hospital (Tehran, Iran.) over 11 months. To accommodate the requirements of autistic subjects that might have prevented signal recording, signals were recorded with a wireless Emotiv Epoch headset device. Use of this device did not produce stress in autistic subjects and this headset was more convenient than other devices because of the short preparation time. The Emotiv Epoch headset is an EEG signal recording device designed to record signals in special conditions such as those found here. The headset has a Bluetooth module for wireless communication. EEG signals were recorded at 14 scalp points according to the international 10–20 system, AF3, AF4, F7, F8, F3, F4, FC6, FC5, T8, T7, P8, P7, O1, O2, and 2 reference electrodes [38, 39]. Fig. 1 a and 1b shows the Emotiv Epoch headset device and electrode placement of electrodes on the scalp.

The Emotiv software was used to record EEG signals and convert them to a MATLAB format [39]. The sampling rate was 128 Hz. A 50-Hz Notch filter was employed to remove the main component of city electricity power and impedance measurements were real-time contact quality using a patented system. Until circles turned green electrodes impedances were decreased using a saline solution. This this indicated that the impedance level required by the software had been achieved.

A Following recording, the artifact free parts of signals (after removal of visual, motion, and EMG artifacts) were selected by a skilled operator under the supervision of a neurologist. The total number of samples recorded during each session, according to the 128 Hz sampling rate, was 18 × 60 × 128 = 138240 samples. In the best conditions this record was obtained in just 50 artifact free five second duration epochs. Ultimately, there were only 50 × 5 ×128 = 32000 samples. Furthermore, during recording no stimuli were used to evoke ERP signals, such as for example, a light flash. In other words, recordings were obtained under relaxed conditions in a calm state and with eyes open, in the absence of any stimulus. All electrode information was obtained as a 14 channel array and this information was read by a MATLAB (Version R2013a) converter program. To prepare the signals, both artifact and city electricity power interference removal was performed. A bandpass finite duration impulse response Hamming window with a cut-off frequency range of 0.5–100 Hz was also used with the MATLAB software [40, 41].

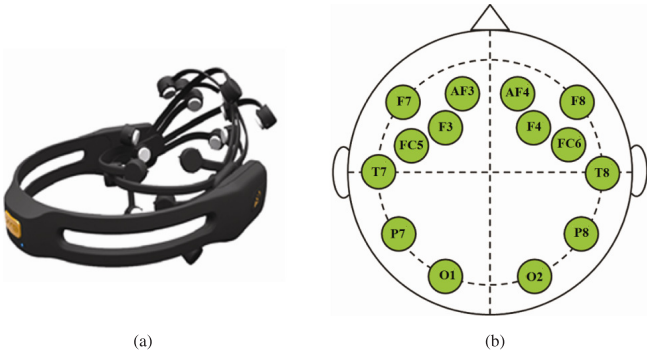

(a) (b)

Fig. 1. (a) Emotiv Epoch headset device, (b) Scalp electrode placement.

2.3. *Feature extraction*

Extracting suitable features from the EEG signals is important. Correct features enable better performance to be achieved by the brain model. Investigations and analyses revealed that the selection of features such as defined by wavelet transform, energy, and entropy from each segment of EEG signal was efficient, provided useful data for the proposed model, and led to good results.

2.3.1. Wavelet transform

The wavelet transform method is more flexible than time-frequency information for windows with different lengths. It is useful for analysis of patterns of irregular data. For EEG signals, the discrete wavelet transform (DWT) was used to analyze the signals of various frequency bands with different resolutions by signal decomposition into coarse, $C_{j,k}$, and detailed, $d_{j,k}$, information. Coefficients were calculated from the following two equations [38, 39]:

$$C_{j,k} = \int_R f(t)\, 2^{-j/2} \overline{\phi\,(2^{-j}t - k)\, dt}, \tag{1}$$

$$d_{j,k} = \int_R f(t)\, 2^{-j/2} \overline{\psi\,(2^{-j}t - k)\, dt}, \tag{2}$$

where $\phi(t)$ is the basic scaling and $\psi(t)$ is the mother wavelet. k is the translation parameter and j is the scale index. Inverse discrete wavelet transforms were calculated as:

$$f(t) = \sum_K C_{j,k} 2^{-j/2} \phi\left(2^{-j}t - k\right) dt + \sum_K d_{j,k} 2^{-j/2} \psi\left(2^{-j}t - k\right) dt. \tag{3}$$

EEG signals were decomposed into five ranges. Electroencephalography recognition requires feature extraction from the acquired signal within the specific frequency ranges of delta, theta, alpha, beta, and gamma [42]. Table 1 shows the bands, which are decomposed into different sub-bands. Next, the energy and entropy from each frequency band was computed.

Table 1. Decomposition of EEG signals into frequency bands

Frequency range	Frequency bands	Frequency bandwidth (Hz)
0–4	Delta	4
4–8	Theta	4
8–16	Alpha	8
16–32	Beta	16
32–64	Gamma	32
64–128	Noise	64

2.3.2. Energy

The relative energy for each decomposition level for the selected epochs of each electrode were calculated. The relative energy quantifies signal strength as it gives the area under the curve as the power within any temporal interval. In signal processing, the energy of a finite EEG signal is given by (4) [38, 39, 43]:

$$E(l) = \sum_{i=1}^{N} d_i^2 \times T/N \tag{4}$$

where N is the number of DWT coefficients d_i at scale l and T is the sampling interval. The relative energy E_r is calculated as:

$$E_r(l) = E(l) / \sum_{i=1}^{S} E(i) \tag{5}$$

where S is the number of wavelet scales.

2.3.3. Entropy

Entropy is a numerical measure of the randomness of a signal. The non-linear characterization of this quantity to measure the complexity of a signal requires the definition of different nonstationary EEG signals. Different types of entropy such as Shannon entropy, log-energy entropy, and Renyi entropy have been proposed for analysis of time-series data. They can discriminate EEG signals into different clinically relevant cases. If the outcome of a probabilistic process is known, the potential reduction of uncertainty can be measured by Shanon entropy. For EEG signals, Shanon entropy measures the average information in the probability distribution of the samples. The Renyi entropy calculates a continuous measure of mutual information. This entropy, in addition to its use in signal analysis, can also be used in ecology and for quantum information calculations. The log-energy entropy quantizes the nonlinear dynamics of EEG signals and defines electrophysiological characters of neurological disease [44]. In this study the entropy at each decomposition level was calculated using [45, 46]:

$$E = -\sum_{j=1}^{N} d_{i,j}^2 \log\left(d_{i,j}^2\right), \tag{6}$$

where i is 1 to l and l shows the wavelet decomposition level. j = 1 to N is the number of coefficients of detail at each decomposition level.

2.4. *Proposed model*

Making a system smart is the important task for artificial intelligence. Therefore, here the inter- and intra-regional connectivity of the brain is presented by use of artificial intelligence. The main aim is to automatically model and present inter- and intra-regional brain connectivity. Previous methods have used only statistical analysis to present inter-region connections and those methods were not able to obtain intra-regional connectivity from EEG signals. However, the present model, based on cellular neural networks, can show the connectivity of various brain regions and also distinguish autistic from non-autistic subjects. The model also accounts for the volume conduction of the human brain. All regions in the model connect with their adjacent and non-adjacent regions and show the connectivity within each region using the features of CNN and electroencephalography.

As mentioned, many regions and cells in the brain connect and react to each other; therefore by considering this aspect, each region (cell) in the model should be affected by and reciprocally affect their adjacent and nonadjacent regions (cells). CNN states and outputs are calculated by the effects of their neighbor's activity. Each cell directly interacts with the cells within its radius of neighborhood, r = 1, and indirectly interacts on the non-neighborhood cells. For this distinguishing property, CNN is used in the brain modeling reported here. The 3D-CNN (two layer CNN) is used to model brain connectivity patterns because, like brain cells, in CNNs the cells connect to and interact with each other. Additionally, using this model to show connective abnormalities of neurophysiological disease is highly efficient and important for the methodologies of biomedical diagnosis.

2.4.1. Cellular neural network

CNNs are information processing systems and act similarly to neural networks. A CNN, like a neural network is a large-scale nonlinear analog circuit that processes input signals from moment to moment [47]. Its dynamic system names locally connecting cells [44]. Features such as continuous-time, parallel processing, immediate signal processing, and local interconnectivity have made the system useful in many scientific fields. These capabilities suited the CNN for numerous applications in the field of pattern recognition [47, 48]. The basic unit of cellular neural networks is called a cell. This unit includes either linear or non-linear elements. Arrays of cells can be configured into different structures. All cells have an input, output, and state. States and outputs are calculated by the effects of neighboring outputs. The connections between cells are referred to as weights, and by using these network dynamics can be greatly increased [48]. As a result of the widespread application area of CNNs and their ability to show the dynamics and operation of complex systems, here a CNN has been used to illustrate the function of a brain region.

2.4.2. The model structure

To make a model of the brain, because the activity within each region may affect other regions, it is important to know the values of the region's connections. Therefore, first the values of a regions connections are calculated using CNN by the structure proposed in Fig. 2. Then, to show the brain intra-region connectivity the structure proposed in Fig. 4 is used.

The Emotiv Epoch has 14 electrodes to record EEG signals; therefore, 14 brain regions are considered. Each region is shown by a cell and here, 14 cells used. Each cell connects to the other 13 cells (each output of the given cell influences all the other cells) so fourteen factorial (14!) connections will be calculated. These connections are inter-regional connections. The ith row and jth column of cells is shown as $C(i, j)$. Lines depicted in Fig. 2 give the links between the cells, which express the interaction of the cells with each other [40, 49].

Each cell is connected to the other 13 cells. Fig. 2a shows the structure of the model that was made by CNN to calculate the inter-region connectivity and Fig. 2b shows the relations of the two electrodes (regions), to the other electrodes (regions). Because drawing all 14! connections in Fig. 2b, was impossible, as an example, only two electrode connections to the other electrodes were drawn, in this figure the relations of AF3 (black arrows) and AF4 (orange arrows) to other cells are given. The arrows between the regions are bidirectional, that is, the regions are reciprocally connected (for example O1 affects O2 and vice versa).

All cells have inputs, outputs, and states. The outputs are calculated by the effect of their neighbor's outputs. Outputs cause cells to communicate with other cells. The states and outputs y_{ij} are defined as [40, 49]:

$$dx_{ij}(t)/dt = -x_{ij}(t) + \sum_{(k,l)\in N(i,j)} A(i,j;k,l)\cdot y_{kl}(t) + \sum_{(k,l)\in N(i,j)} B(i,j;k,l)\cdot u_{kl}(t) + z(i,j;k,l), \tag{7}$$

$$y_{ij} = f\left(x_{ij}(t)\right) = (1/2)\left(\left|x_{ij}(t)+1\right| - \left|x_{ij}(t)-1\right|\right) \tag{8}$$

where f is a nonlinear function. Note that it is possible to use other suitable functions for f [40, 49].

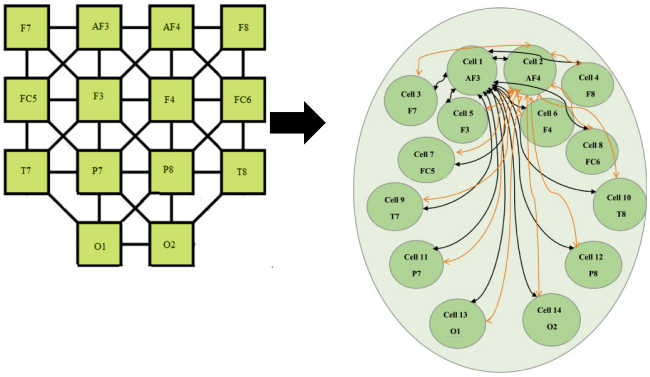

(a) (b)

Fig. 2. Model employed for calculation of the inter-regional connection values: (a) structure of the proposed CNN model containing 14 cells, (b) Example of the inter-region connectivity for electrodes AF3 and AF4.

After calculating the values of the connections between regions, in the second step, a 3D 4×4 CNN is used to show the intra-region connections within each region. Using the CNNs in each brain region by considering the connections of the regions (connections obtained by the model in Fig. 2 generates a model that putatively works like a brain. Here, the 3D 4×4 CNN has been used as an example to represent the intra-region connections of each region. Each suitable structure of the CNN can be used (for example 3×3, 5×5 and ...CNNs). In fact, using large CNNs with many dimensions gives greater similarity to the brains regions, but to reduce computational complexity, the present study used 4×4 CNNs. Fig. 3 shows the structure of the 3D-CNN used to model a region. The *i*th row, *j*th column and *k*th dimension of cells is shown as *C(i, j, k)*. For example, C3, 2, 2 shows the cell in row three, column two, and dimension two. Lines depicted in Fig. 3 show the links between the cells, which express the interaction of the cells with each other [40, 49].

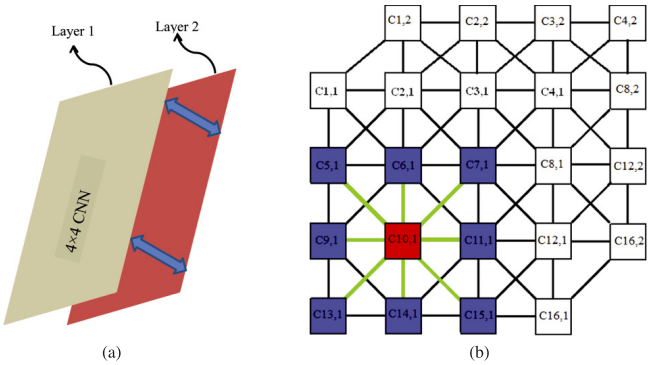

(a) (b)

Fig. 3. (a) Two layers of a 3D-CNN, (b) Display of connections between cells in a 3D-CNN.

The values associated with the links of the cells, show the value of the intra-region connections in each region. Each cell has an input, output, and state. Cells communicate with other cells via their outputs. The state of cell is the weighted sum of its inputs. The state of the cell (i, j, k) is given by [40, 49]:

$$dx_{ijk}(t)/dt = -x_{ijk}(t) + \sum_{(f,l,k)\in N(i,j,k)} A(i,j,k;f,l,k)\cdot y_{flk}(t) + \sum_{(f,l,k)\in N(i,j,k)} B(i,j,k;f,l,k)\cdot u_{flk}(t) + z(i,j,k;f,l,k), \quad (9)$$

where u, x, and y are the input, state, and output of the cell i, j, and k, respectively; f and l are the indices belonging to the neighboring cell $N(i, j, k)$ of the cell (i, j, k). All the variables are continuous. The set of matrices and the threshold A, B, z, which contains the weights of the neural nonlinear network, defines the operation performed by the network. The output y_{ijk} is defined as [40, 49]:

$$y_{ijk} = f\left(x_{ijk}(t)\right) = (1/2)\left(\left|x_{ijk}(t)+1\right| - \left|x_{ijk}(t)-1\right|\right). \quad (10)$$

The model proposed shows the inter- and intra-regional connections of an individuals' brain regions by CNN. According to the main regions of the brain and the electrodes, which recorded the signals from each region, a unique structure was designed. This structure contained as main regions, the frontal, parietal, temporal, and occipital lobes of the left and right brain hemispheres. Fig. 4 shows the complete model structure.

As is seen, each square represents a region of the brain that is simulated by a 3D 4×4 CNN. All cells in a CNN are connected with their neighbors. Each region has a relationship with its adjacent and non-adjacent regions. For instance, the relationships of the AF4 region (black arrows) and the AF3 region (orange arrows), to the other regions have been shown in Fig. 4 (for all regions, arrows should be drawn because they all connect with each other). Arrows between regions are bidirectional, that is, the regions interact with each other (for example O1 affects O2, and vice versa).

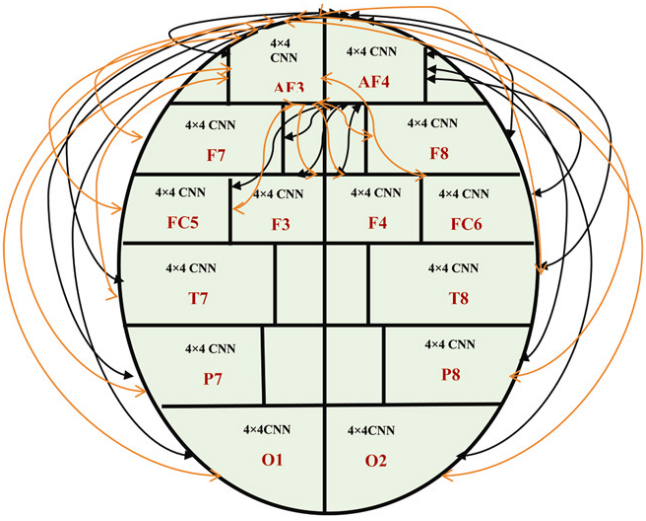

Fig. 4. Structure for intra-region connectivity in the presented model.

As mentioned, the value of connections between non-adjacent regions have been calculated by the model and are given in Fig. 2. After employing extracted features as inputs, intra-regional connections of the brain as illustrated by the proposed model in Fig. 4. This model is extended such that it is possible to use it to compute and consider relations between inter- and intra-regional connections.

Table 2. Average energy and entropy values of the alpha band EEG for non-autistic and ASD subjects

Electrodes	Energy*			Entropy+		
	ASD subjects (mean ± SD)	Non-autistic subjects (mean ± SD)	*P* value	ASD subjects (mean ± SD)	Non-autistic subjects (mean ± SD)	*P* value
AF3	0.8001 ± 0.13	0.9998 ± 0.11	0.13	0.7502 ± 0.17	0.7198 ± 0.12	*0.41*
AF4	0.8549 ± 0.21	0.8952 ± 0.11	0.87	0.8411 ± 0.15	0.8001 ± 0.21	*0.11*
F3*+	0.7489 ± 0.05	0.9521 ± 0.03	0.00	0.5829 ± 0.11	0.7422 ± 0.18	0.00
F4	0.9522 ± 0.24	0.8542 ± 0.14	0.58	0.6103 ± 0.13	0.6996 ± 0.21	0.21
F7+	0.7952 ± 0.36	0.8501 ± 0.23	0.48	0.6021 ± 0.19	0.8023 ± 0.15	0.00
F8	0.8174 ± 0.38	0.8949 ± 0.14	0.91	0.751 ± 0.23	0.7891 ± 0.14	0.53
FC6	0.9685 ± 0.13	0.9105 ± 0.21	0.82	0.8523 ± 0.21	0.8505 ± 0.15	*0.49*
FC5+	0.9600 ± 0.26	0.9258 ± 0.15	0.71	0.8512 ± 0.13	0.9051 ± 0.11	0.05
T7*	0.9745 ± 0.09	0.7935 ± 0.09	0.05	0.8530 ± 0.09	0.7935 ± 0.09	0.05
T8	0.8925 ± 0.31	0.8859 ± 0.24	0.92	0.7041 ± 0.12	0.7680 ± 0.15	0.71
P7*+	0.9003 ± 0.04	0.8257 ± 0.02	0.02	0.8102 ± 0.13	0.931 ± 0.01	0.05
P8	0.7859 ± 0.12	0.8296 ± 0.14	0.70	0.9021 ± 0.18	0.9905 ± 0.12	0.27
O1*+	0.6103 ± 0.11	0.8196 ± 0.15	0.01	0.6103 ± 0.13	0.8196 ± 0.15	0.01
O2	0.7372 ± 0.12	0.8009 ± 0.18	0.79	0.5413 ± 0.14	0.6126 ± 0.11	0.09

2.5. *Statistical analysis*

To demonstrate differences, the data obtained and results of the proposed model should be analyzed by statistical testing. Here, the comparisons used included two-tailed tests (*t*-test) with a 95% confidence interval. Probability values (p) less than 0.05 were considered as statistically significant [17, 50].

3. Results and discussion

This study was conducted using MATLAB R2013a. First, recorded signals were pre-processed and signal noise minimized. Then all mentioned features were extracted from non-autistic and autistic signals which were then applied as inputs to the given network model. To visualize and compare patterns within each group, input values obtained for each group were separately applied to the model. For CNNs, the values of states and outputs (connections) are important, therefore in this study these values were reported for the applied input patterns and differences.

Prior to using the model, energy and entropy values of the signals for two groups are presented. Because significant differences were observed in alpha band, the mean and standard deviation (mean ± SD) of those values, for the two subject groups, in alpha band are summarized in Table 2. Significant differences for energy and entropy are marked with $*$ and $+$, respectively in Table 2.

It was observed that, there were significant differences in energy values obtained from four electrodes (F3, T7, P7, and O1), whereas, the entropy values were significant for somewhat different electrodes (F3, F7, FC5, and O1). Based on these analyses, separating the two groups was difficult and indicated that connectivity pattern differences were impossible; therefore, the differences are reported by the proposed model. In fact, the main purpose of this paper is to automatically present the inter- and intra-region connections of the brain by the unique model.

The model will be used to show the connections between the various regions of the brain. All input cells, based on the input feature vectors and effects of their neighbors output values, calculate their own output and state values. The connectivity between cells are the same as the cell outputs. In Table 3 the connection values of the three bands: alpha, beta, and gamma, are presented using the model in Fig. 2. As mentioned, 14! connections should be calculated. As such a Table is too long, only some values are reported. The values obtained indicate the inter-region connectivity values and are used in the continuation experiment for intra-region connections. Significant differences in the table are marked with an asterisk (*) for the alpha (α), beta (β), and gamma (γ) bands.

Calculation of CNN values to find the connectivity between electrode pairs in the brain illustrated that more abnormalities are related to the connectivity of the temporal lobes than with other lobes in the gamma band. Lower values between the temporal lobes and other lobes can be interpreted as a reflection of a genuinely decreased correlation of cortical activities. It was observed there were abnormalities and higher valued connections in distant electrodes in autistic subjects for all three bands, especially the gamma band. Additionally, abnormalities in the connection values of neighboring electrodes were also observed. Results confirm this hypothesis. Although the autistic brain is healthy, there are abnormalities in the organization and connectivity of its regions [8, 15, 16].

The intra-regions connections are accounted for by the states of and connections between the cells. The state values show the condition of each cell based on the input value and influence of its neighboring output values. It should be noted that each region contains 32 cells ($C_{i,j,k}$). Hence, 32 states are present for each electrode (region). 16 cells and states for dimension one and 16 cells and states for dimension two. S represents the state and $C_{1,1,1}$, $C_{1,2,1}$, $C_{1,3,1}$, $C_{1,4,1}$, $C_{2,1,1}$, $C_{2,2,1}$, $C_{2,3,1}$, $C_{2,4,1}$, $C_{3,1,1}$, $C_{3,2,1}$, $C_{3,3,1}$, $C_{3,4,1}$, $C_{4,1,1}$, $C_{4,2,1}$, $C_{4,3,1}$, $C_{4,4,1}$, $C_{1,1,2}$, $C_{1,2,2}$, $C_{1,3,2}$, $C_{1,4,2}$, $C_{2,1,2}$, $C_{2,2,2}$, $C_{2,3,2}$, $C_{2,4,2}$, $C_{3,1,2}$, $C_{3,2,2}$, $C_{3,3,2}$, $C_{3,4,2}$, $C_{4,1,2}$, $C_{4,2,2}$, $C_{4,3,2}$ and $C_{4,4,2}$, produce $S_{1,1}$, $S_{2,1}$, $S_{3,1}$, $S_{4,1}$, $S_{5,1,2}$, $S_{6,1,2}$, $S_{7,1,2}$, $S_{8,1}$, $S_{9,1}$, $S_{10,1}$, $S_{11,1}$, $S_{12,1}$, $S_{13,1}$, $S_{14,1}$, $S_{15,1}$, $S_{16,1}$, $S_{1,2}$, $S_{2,2}$, $S_{3,2}$, $S_{4,2}$, $S_{5,2}$, $S_{6,2}$, $S_{7,2}$, $S_{8,2}$, $S_{9,2}$, $S_{10,2}$, $S_{11,2}$, $S_{12,2}$, $S_{13,2}$, $S_{14,2}$, $S_{15,2}$ and $S_{16,2}$, respectively.

There are 14 electrodes, therefore 14 Tables should be written. Table 4 gives the average state values obtained in the alpha band from electrode F3 for 100 non-autistic and ASD subjects. Based on the analysis, significant differences are marked with an asterisk (*) in Table 4.

Table 3. Average connection values obtained for EEG in α, β and γ bands, for 100non-autistic subjects and ASD subjects based on the model in Fig. 2 for electrode pairs

Electrodes	Energy*			Entropy+					
	ASD subjects (mean ± SD)	Non-autistic subjects (mean ± SD)	*P* value	ASD subjects (mean ± SD)	Non-autistic subjects (mean ± SD)	*P* value	ASD subjects (mean ± SD)	Non-autistic subjects (mean ± SD)	*P* value
F7–F8	0.521 ± 0.15	0.592 ± 0.16	0.37	0.631 ± 0.25	0.682 ± 0.10	0.29	0.721 ± 0.11	0.758 ± 0.01	0.21
F7–T8$^{\times+*}$	0.308 ± 0.11	0.338 ± 0.09	0.05	0.385 ± 0.13	0.391 ± 0.09	0.05	0.408 ± 0.01	0.658 ± 0.06	0.00
F7–F3	0.411 ± 0.27	0.444 ± 0.19	0.48	0.490 ± 0.12	0.501 ± 0.16	0.31	0.511 ± 0.21	0.594 ± 0.24	0.78
F7–O1$^{\times+*}$	0.307 ± 0.09	0.381 ± 0.07	0.01	0.385 ± 0.08	0.409 ± 0.03	0.03	0.415 ± 0.05	0.682 ± 0.012	0.00
F7–O2^{+*}	0.375 ± 0.18	0.382 ± 0.11	0.25	0.495 ± 0.07	0.562 ± 0.12	0.02	0.465 ± 0.08	0.612 ± 0.02	0.00
T8–FC5*	0.485 ± 0.15	0.501 ± 0.27	0.38	0.511 ± 0.17	0.525 ± 0.18	0.27	0.517 ± 0.02	0.631 ± 0.04	0.01
F8–O1*	0.315 ± 0.11	0.342 ± 0.21	0.19	0.421 ± 0.17	0.423 ± 0.19	0.41	0.315 ± 0.00	0.521 ± 0.09	0.00
F8–P7*	0.201 ± 0.22	0.253 ± 0.15	0.21	0.341 ± 0.12	0.401 ± 0.00	0.32	0.281 ± 0.02	0.478 ± 0.00	0.00
F8–O2$^{\times*}$	0.482 ± 0.08	0.553 ± 0.05	0.05	0.677 ± 0.13	0.692 ± 0.11	0.24	0.552 ± 0.03	0.752 ± 0.01	0.00
F8–O1*	0.351 ± 0.21	0.368 ± 0.31	0.52	0.398 ± 0.32	0.407 ± 0.18	0.18	0.472 ± 0.02	0.500 ± 0.03	0.05
F3–T7$^{\times+*}$	0.452 ± 0.13	0.505 ± 0.07	0.05	0.537 ± 0.19	0.598 ± 0.09	0.04	0.492 ± 0.03	0.675 ± 0.01	0.00
AF3–AF4	0.467 ± 0.19	0.481 ± 0.25	0.42	0.499 ± 0.17	0.508 ± 0.19	0.24	0.581 ± 0.21	0.601 ± 0.13	0.15
P7–P8	0.402 ± 0.09	0.421 ± 0.22	0.21	0.452 ± 0.29	0.780 ± 0.13	0.19	0.492 ± 0.13	0.500 ± 0.02	0.10
P8–O2	0.489 ± 0.12	0.504 ± 0.21	0.29	0.511 ± 0.28	0.543 ± 0.22	0.36	0.519 ± 0.18	0.594 ± 0.11	0.37

Table 4. Average state values obtained for electrode F3 for 100 Non-autistic and ASD subjects in the α band

States ASD subjects	(mean ± SD)	Non-autistic subjects (mean ± SD)	Statistical analysis (*p* value)
S1, 1	0.135 ± 0.004	0.728 ± 0.025	0.00
S2, 1*	0.034 ± 0.012	0.652 ± 0.007	0.00
S3, 1*	0.754 ± 0.051	0.847 ± 0.013	0.05
S4, 1*	0.7213 ± 0.001	0.8206 ± 0.086	0.00
S5, 1*	0.036 ± 0.023	0.7879 ± 0.007	0.00
S6, 1*	0.064 ± 0.049	0.7857 ± 0.002	0.00
S7, 1*	0.851 ± 0.010	0.6274 ± 0.028	0.00
S8, 1*	0.8233 ± 0.096	0.9340 ± 0.090	0.01
S9, 1*	0.01 ± 0.002	0.899 ± 0.003	0.00
S10, 1*	0.086 ± 0.011	0.8153 ± 0.021	0.00
S11, 1*	0.872 ± 0.006	0.9542 ± 0.027	0.05
S12, 1	0.8651 ± 0.050	0.815 ± 0.010	0.10
S13, 1*	0.026 ± 0.009	0.712 ± 0.004	0.00
S14, 1*	0.321 ± 0.034	0.7142 ± 0.049	0.00
S15, 1*	0.6317 ± 0.021	0.7121 ± 0.043	0.00
S16, 1*	0.6129 ± 0.023	0.7108 ± 0.015	0.00
S1, 2*	0.234 ± 0.014	0.728 ± 0.025	0.00
S2, 2*	0.041 ± 0.003	0.642 ± 0.010	0.00
S3, 2*	0.739 ± 0.051	0.856 ± 0.012	0.05
S4, 2*	0.621 ± 0.003	0.8316 ± 0.006	0.00
S5, 2*	0.046 ± 0.023	0.8870 ± 0.015	0.00
S6, 2*	0.068 ± 0.059	0.7857 ± 0.002	0.00
S7, 2*	0.951 ± 0.013	0.6814 ± 0.028	0.00
S8, 2*	0.7523 ± 0.086	0.9040 ± 0.081	0.01
S9, 2*	0.0152 ± 0.021	0.898 ± 0.005	0.00
S10, 2*	0.0812 ± 0.001	0.8853 ± 0.021	0.00
S11, 2*	0.851 ± 0.010	0.9042 ± 0.024	0.05
S12, 2	0.8532 ± 0.050	0.835 ± 0.012	0.10
S13, 2*	0.028 ± 0.006	0.692 ± 0.010	0.00
S14, 2*	0.425 ± 0.0246	0.6940 ± 0.047	0.00
S15, 2*	0.6517 ± 0.021	0.7321 ± 0.032	0.00
S16, 2*	0.5999 ± 0.033	0.7517 ± 0.013	0.00

Table 5. Average state values obtained for electrode F4 for 100 Non-autistic and ASD subjects in α band

States ASD subjects	(mean ± SD)	Non-autistic subjects (mean ± SD)	Statistical analysis (*p* value)
S1, 1	0.931 ± 0.004	0.9385 ± 0.007	0.700
S2, 1	0.9042 ± 0.004	0.9065 ± 0.002	0.900
S3, 1	0.927 ± 0.080	0.812 ± 0.086	0.175
S4, 1	0.7175 ± 0.232	0.7340 ± 0.256	0.700
S5, 1	0.5832 ± 0.229	0.5852 ± 0.171	0.893
S6, 1	0.4501 ± 0.060	0.5627 ± 0.065	0.168
S7, 1	0.4615 ± 0.123	0.4367 ± 0.111	0.129
S8, 1	0.9352 ± 0.052	0.9475 ± 0.004	0.220
S9, 1	0.9427 ± 0.015	0.9552 ± 0.020	0.685
S10, 1	0.9380 ± 0.021	0.9645 ± 0.018	0.503
S11, 1	0.9692 ± 0.016	0.9917 ± 0.028	0.124
S12, 1	0.8637 ± 0.014	0.8877 ± 0.099	0.129
S13, 1*	0.9340 ± 0.012	0.713 ± 0.121	0.003
S14, 1	0.952 ± 0.042	0.955 ± 0.044	0.985
S15, 1	0.9585 ± 0.041	0.9465 ± 0.034	0.542
S16, 1	0.822 ± 0.192	0.802 ± 0.173	0.614
S1, 2	0.946 ± 0.012	0.9781 ± 0.021	0.690
S2, 2	0.9851 ± 0.012	0.9171 ± 0.007	0.900
S3, 2	0.951 ± 0.079	0.849 ± 0.047	0.751
S4, 2	0.8001 ± 0.341	0.7591 ± 0.301	0.700
S5, 2	0.6002 ± 0.301	0.5592 ± 0.261	0.798
S6, 2	0.5521 ± 0.100	0.5701 ± 0.059	0.171
S7, 2*	0.2930 ± 0.102	0.5420 ± 0.091	0.001
S8, 2	0.9131 ± 0.042	0.9245 ± 0.012	0.581
S9, 2	0.9801 ± 0.018	0.9121 ± 0.019	0.710
S10, 2	0.9210 ± 0.012	0.9352 ± 0.009	0.611
S11, 2	0.9312 ± 0.014	0.9885 ± 0.015	0.201
S12, 2	0.8995 ± 0.101	0.8531 ± 0.015	0.200
S13, 2*	0.8992 ± 0.101	0.658 ± 0.111	0.004
S14, 2	0.941 ± 0.031	0.972 ± 0.024	0.945
S15, 2	0.9320 ± 0.045	0.9585 ± 0.071	0.795
S16, 2	0.822 ± 0.192	0.801 ± 0.175	0.614

Table 6. States that have significantly different values ($p < 0.05$) for 14 channels between non-autistic and ASD subjects in α, β, and γ bands

Region	α band	β band	γ band
AF3	All 32 states	S5, 1, S6, 1, S7, 1, S8, 1, S10, 1, S11, 1, S12, 1, S14, 1, S15, 1, S1, 2, S4, 2, S5, 2, S6, 2, S7, 2, S8, 2, S10, 2, S11, 2, S12, 2, S14, 2, S15, 2	S5, 1, S6, 1, S7, 1, S8, 1, S10, 1, S11, 1, S12, 1, S14, 1, S15, 1, S1, 2, S6, 2, S7, 2, S8, 2, S10, 2, S11, 2, S12, 2, S14, 2, S15, 2
AF4	S1, 1, S4, 1, S5, 1, S6, 1, S7, 1, S8, 1, S10, 1, S11, 1, S12, 1, S14, 1, S15, 1, S1, 2, S4, 2, S5, 2, S6, 2, S7, 2, S8, 2, S10, 2, S11, 2, S12, 2, S14, 2, S15, 2	S14, 1, S15, 1, S1, 2, S6, 2, S7, 2, S8, 2, S10, 2, S11, 2, S12, 2, S14, 2, S15, 2, S16, 2	S1, 1, S4, 1, S5, 1, S6, 1, S11, 2, S12, 2
F3	S1, 1, S2, 1, S3, 1, S4, 1, S5, 1, S6, 1, S7, 1, S9, 1, S10, 1, S11, 1, S13, 1, S14, 1, S15, 1, S16, 1, S1, 2, S2, 2, S3, 2, S4, 2, S5, 2, S6, 2, S7, 2, S9, 2, S10, 2, S11, 2, S13, 2, S14, 2, S15, 2, S16, 2	S2, 1, S3, 1, S4, 1, S5, 1, S6, 1, S7, 1, S9, 1, S10, 1, S11, 1, S13, 1, S14, 1, S15, 1, S16, 1, S1, 2, S2	S15, 1, S16, 1, S1, 2, S2, 2, S3, 2, S4, 2, S5, 2, S6, 2, S7, 2, S9, 2, S10, 2, S11, 2, S13, 2, S14, 2, S15, 2, S16, 2
F4	S7, 1, S13, 1, S7, 2, S13, 2	No states	S3, 2
F7	S1, 1, S5, 1, S6, 1, S7, 1, S10, 1, S11, 1, S15, 1, S1, 2, S5, 2, S6, 2, S7, 2, S10, 2, S11, 2, S15, 2	S6, 2, S7, 2	S14, 1, S15, 1, S16, 1, S1, 2, S2, 2, S3, 2, S4, 2, S5, 2, S6, 2, S7, 2
F8	S11, 1, S12, 1, S11, 2, S12, 2	No states	No states
FC6	S12, 1, S5, 1, S12, 2, S5, 2	S7, 2, S9, 2	S15, 1
FC5	S1, 1, S2, 1, S3, 1, S12, 1, S14, 1, S1, 2, S2, 2, S3, 2, S12, 2, S14, 2	S14, 1, S15, 1, S1, 2, S6, 2, S7, 2, S8, 2, S10, 2, S11, 2	S10, 1, S11, 1, S13, 1, S14, 1, S14, 2, S15, 2, S16, 2
T7	S1, 1, S2, 1, S6, 1, S7, 1, S8, 1, S9, 1, S11, 1, S12, 1, S13, 1, S1, 2, S2, 2, S6, 2, S7, 2, S8, 2, S9, 2, S11, 2, S12, 2, S13, 2	S10, 1, S11, 1, S13, 1, S14, 1, S15, 1, S16, 1, S1, 2, S2, 2, S3, 2, S4, 2, S5, 2, S6, 2, S7, 2, S9, 2, S10, 2, S11, 2, S13, 2	S11, 1, S13, 1, S14, 1, S15, 1, S16, 1, S1, 2, S2, 2, S3, 2, S5, 2, S6, 2, S7, 2, S9, 2, S10, 2, S11, 2
T8	No states	No states	No states
P7	All 32 states	S1, 1, S2, 1, S3, 1, S4, 1, S5, 1, S8, 1, S9, 1, S10, 1, S11, 1, S2, 2, S3, 2, S4, 2, S5, 2, S8, 2, S9, 2, S10, 2, S11, 2, S13, 2, S14, 2, S16, 2	S1, 2, S2, 2, S3, 2, S4, 2, S5, 2, S6, 2, S7, 2, S9, 2, S10, 2, S11, 2, S13, 2, S14, 2, S15, S14, 2, S16, 2
P8	S11, 1, S15, 1, S16, 1, S11, 2, S15, 2, S16, 2	No states	No states
O1	S1, 1, S2, 1, S3, 1, S4, 1, S5, 1, S8, 1, S9, 1, S10, 1, S11, 1, S13, 1, S14, 1, S16, 1, S1, 2, S2, 2, S3, 2, S4, 2, S5, 2, S8, 2, S9, 2, S10, 2, S11, 2, S13, 2, S14, 2, S16, 2	S5, 1, S6, 1, S7, 1, S8, 1, S10, 1, S11, 1, S12, 1, S14, 1, S15, 1, S1, 2, S6, 2, S7, 2, S8, 2, S10, 2, S11, 2, S12, 2, S14, 2, S15, 2	S2, 1, S3, 1, S4, 1, S5, 1, S6, 1, S7, 1, S9, 1, S10, 1, S11, 1, S13, 1, S14, 1, S16, 1, S1, 2, S2, 2, S3, 2, S4, 2, S5, 2, S6, 2, S7, 2, S9, 2, S10, 2, S11, 2, S13, 2, S14, 2, S15, 2
O2	S4, 1, S7, 1, S4, 2, S7, 2	S13, 1	S11, 1

Table 7. Average values obtained for connection weights for 100 autistic and non-autistic subjects in 14 region for α, β, and γ bands

Electrodes	Energy*			Entropy+					
	ASD subjects (mean ± SD)	Non-autistic subjects (mean ± SD)	*P* value	ASD subjects (mean ± SD)	Non-autistic subjects (mean ± SD)	*P* value	ASD subjects (mean ± SD)	Non-autistic subjects (mean ± SD)	*P* value
AF3$^{\times+*}$	0.499 ± 0.03	0.978 ± 0.02	0.00	0.408 ± 0.09	0.828 ± 0.11	0.00	0.521 ± 0.09	0.988 ± 0.12	0.00
AF4$^{\times}$	0.541 ± 0.033	0.925 ± 0.040	0.00	0.822 ± 0.13	0.878 ± 0.19	0.24	0.901 ± 0.09	0.910 ± 0.07	0.15
F3$^{\times}$	0.740 ± 0.03	0.952 ± 0.04	0.00	0.759 ± 0.18	0.9672 ± 0.09	0.00	0.851 ± 0.13	0.952 ± 0.04	0.00
F4	0.752 ± 0.19	0.693 ± 0.16	0.48	0.789 ± 0.08	0.709 ± 0.14	0.31	0.801 ± 0.09	0.733 ± 0.21	0.28
F7$^{\times+}$	0.497 ± 0.004	0.608 ± 0.121	0.052	0.499 ± 0.07	0.572 ± 0.13	0.03	0.625 ± 0.18	0.642 ± 0.10	0.31
F8	0.583 ± 0.13	0.704 ± 0.16	0.12	0.661 ± 0.11	0.714 ± 0.19	0.15	0.683 ± 0.17	0.744 ± 0.12	0.13
FC6	0.799 ± 0.02	0.804 ± 0.06	0.34	0.805 ± 0.09	0.814 ± 0.16	0.21	0.899 ± 0.12	0.902 ± 0.09	0.11
FC5	0.865 ± 0.13	0.895 ± 0.05	0.17	0.897 ± 0.14	0.905 ± 0.17	0.24	0.906 ± 0.13	0.966 ± 0.05	0.29
T7$^{\times+*}$	0.605 ± 0.08	0.773 ± 0.03	0.01	0.637 ± 0.07	0.692 ± 0.07	0.03	0.652 ± 0.03	0.752 ± 0.11	0.01
T8	0.647 ± 0.18	0.630 ± 0.34	0.69	0.697 ± 0.11	0.699 ± 0.31	0.49	0.700 ± 0.21	0.705 ± 0.32	0.37
P7$^{\times+*}$	0.563 ± 0.036	0.836 ± 0.044	0.00	0.589 ± 0.12	0.904 ± 0.21	0.02	0.571 ± 0.09	0.943 ± 0.12	0.01
P8	0.904 ± 0.03	0.927 ± 0.03	0.17	0.913 ± 0.10	0.920 ± 0.12	0.11	0.934 ± 0.06	0.937 ± 0.03	0.17
O1$^{\times}$	0.805 ± 0.02	0.829 ± 0.05	0.13	0.817 ± 0.14	0.829 ± 0.10	0.05	0.819 ± 0.02	0.889 ± 0.01	0.04
O2	0.538 ± 0.02	0.549 ± 0.03	0.58	0.551 ± 0.28	0.543 ± 0.22	0.36	0.579 ± 0.22	0.594 ± 0.11	0.12

Table 5 gives the average values obtained in the α band from electrode F4 for 100 non-autistic and ASD subjects. As seen in this Table, only three states show any significant difference between any two groups.

The state values obtained from autistic subjects when compared with non-autistic subjects in Tables 4 and 5, indicate differences exist between non-autistic and autistic subjects in the anterior-frontal region (F3); however, in the F4 region, no significant differences

Table 8. Average values of intra-regional connectivity in each brain lobe for 100 autistic and non-autistic subjects in the alpha band Right hemisphere Left hemisphere

The lobes	Right hemisphere			Left hemisphere		
	ASD subjects (mean ± SD)	Non-autistic subjects (mean ± SD)	Statistical analysis (mean ± SD)	ASD subjects (mean ± SD)	Non-autistic subjects (mean ± SD)	Statistical analysis
Frontal	0.647 ± 0.171	0.853 ± 0.149	0.028	0.666 ± 0.189	0.780 ± 0.099	0.054
Temporal	0.676 ± 0.080	0.769 ± 0.031	0.011	0.657 ± 0.198	0.630 ± 0.998	0.731
Parietal	0.563 ± 0.036	0.941 ± 0.044	0.00	0.956 ± 0.029	0.977 ± 0.031	0.177
Occipital	0.881 ± 0.023	0.888 ± 0.051	0.105	0.538 ± 0.024	0.538 ± 0.022	0.991

were observed. It is concluded that there are significant differences in the activity of brain regions in subjects with autism compared to non-autistic subjects.

Table 6 shows the states that have significant differences for the 14 regions studied. In this Table only the states that have significant differences ($p < 0.05$) in α, β, and γ bands, between non-autistic and ASD subjects have been given.

The state values obtained and reported in Table 6, indicated that for all three bands there were significant differences in the value of the states of the autistic brain in parts of the left hemisphere and anterior-frontal regions. In the alpha band, more differences were observed in the states of the left hemisphere of the autistic brain.

Table 7 reports the average connection values for each region for 100 non-autistic and autistic subjects in three bands α, β, and γ. Significant differences in values between two groups are marked with $\times$, $+$, and $*$, in Table 7.

According to the values obtained, significant differences were observed in the in alpha band of regions related to the AF3, AF4, F3, P7, T7, F7, and O1 electrodes of subjects with autism when compared to non-autistic subjects. Additionally, in AF3, F7, T7, and P7 significant differences were observed in the beta band and for P7 and T7 in the gamma band. Results showed that most abnormalities in subjects with autism are related to the left hemisphere of the brain, especially the frontal and temporal lobes. The results obtained are in agreement with reports by Rashidi and Sheikhani [5, 17, 51]. On the basis of Tables 6 and 7, it can be concluded that abnormalities are observed in the left hemisphere of autistic subjects. To support this hypothesis, the intra-regional connectivity of the lobes in the left and right hemispheres for autistic and non-autistic subjects in the alpha band are presented in Table 8. This Table shows the average connectivity values of the intraregional connections in each lobe.

Table 8 shows significant differences in the left hemisphere of subjects with autism compared to non-autistic subjects. However, no significant differences was observed in the right hemisphere.

In this study, two types of significant differences were found between the two groups. The first was the difference in activity of the regions in the frontal and left hemisphere of the brain and the differences are shown by state. The second was the connectivity differences of the inter- and intra-regions calculated for cell outputs. The results obtained match those reported by Behnam, Sheikhani, Vissers and Barttfeld [5, 50–52].

The main purpose of the present model is to show brain region connectivity. This model was able to distinguish two groups using the 3D-CNN values obtained, which demonstrates the practicality of the model. The model proposed showed differences for electrodes F3, AF3, AF4, F7, P7, O1 and T7 in the alpha band, at electrodes AF3, F7, T7, P7 in the beta band, and for electrodes P7 and T7 in the gamma band in the frontal lobe and left hemisphere of autistic subjects when compared to normal subjects. The model based on the state values and the weights obtained from the CNNs distinguish these two groups via a support vector machine (SVM). SVM is a classifier that can separate different types of EEG signal [44]. It is a non-linear binary classifier, which maps the input features (here the state and weight values) onto a higher dimensional hyper-plane. The best hyper-plane was used to separate the data points of one class from the other to classify the signals. In this paper, the performance of the SVM classifier was measured using a third order polynomial kernel function with 0.8592 and 0.8972, sensitivity and specificity, respectively. Here, tenfold cross-validation was used to improve accuracy. Evaluation of the analysis demonstrated that the alpha frequency band had the best distinction capacity (96.6%) and shows the precision of the model proposed.

4. Conclusion

This paper has presented a model to show the brain connectivity of children with autism using features of electroencephalography and 3D-cellular neural networks. The cellular neural network was found to be a suitable tool to model the connections and differences between autistic and non-autistic patterns in the different regions. Results illustrated that more abnormalities are related to the left hemisphere, ($p < 0.05$) at electrode locations AF3, F3, P7, T7, and O1, in the alpha band, and AF3, F7, T7, and O1 in the beta band, and T7 and P7 in the gamma band for children with autism when compared with a non-autistic group. Evaluation of the connection values obtained for different brain regions indicated that there are more abnormalities in the connectivity of frontal and parietal lobes and the relations of the neighboring regions in all three bands, especially in the gamma band, for autistic children. The model also distinguished autistic and non-autistic subjects with an accuracy rate of 96.6% in the alpha band from the state and weight values obtained using SVM. Results confirmed the hypothesis that, although the autistic brain is healthy there are abnormalities in the organization and connectivity of its regions. Some limitations of this study merit consideration. First, children with autism could not be sat for a long time. Moreover, for the EEG they could not avoid taking their medication for a long time. Future work could be to distinguish ASD girls and boys using this model. Also, brain inter- and intra-region connections of ASD girls and boys in different EEG bands could be compared and discussed.

Acknowledgments

None.

Conflict of Interest

All authors declare no conflicts of interest.

References

[1] Mason RA, Williams DL, Kana RK, Minshew N, Just MA (2008) Theory of Mind disruption and recruitment of the right hemisphere during narrative comprehension in autism. *Neuropsychologia* **46(1)**, 269-280.

[2] Perkins TJ, Stokes MA, Mcgillivray JA, Mussap AJ, Cox IA, Maller JJ, Bittar RG (2014) Increased left hemisphere impairment in high-functioning autism: a tract based spatial statistics study. *Psychiatry Research Neuroimaging* **224(2)**, 119-123.

[3] Johansen-Berg H, Rushworth MFS (2009) Using Diffusion Imaging to Study Human Connectional Anatomy. *Annual Review of Neuroscience***32(1)**, 75-94.

[4] Buckner RL, Andrewshanna JR, Schacter DL (2008) The brain's default network: anatomy, function, and relevance to disease. *Annals of the New York Academy of Sciences* **1124(1)**, 1-38.

[5] Vissers ME, Cohen MX, Geurts HM (2012) Brain connectivity and high functioning autism: A promising path of research that needs refined models, methodological convergence, and stronger behavioral links. *Neuroscience & Biobehavioral Reviews* **36(1)**, 604-625.

[6] Assaf M, Jagannathan K, Calhoun VD, Miller L, Stevens MC, Sahl R, O'Boyle JG, Schultz RT, Pearlson GD (2010) Abnormal functional connectivity of default mode sub-networks in autism spectrum disorder patients. *Neuroimage* **53(1)**, 247-256.

[7] Weng SJ, Wiggins JL, Peltier SJ, Carrasco M, Risi S, Lord C, Monk CS (2010) Alterations of resting state functional connectivity in the default network in adolescents with autism spectrum disorders. *Brain Research* **1313**, 202-214.

[8] Kennedy DP, Courchesne E (2008) The intrinsic functional organization of the brain is altered in autism. *Neuroimage* **39(4)**, 1877-1885.

[9] Kanner L (1943) Autistic disturbances of affective contact. *Acta Paedopsychiatr* **35(4)**, 100-136.

[10] Sheikhani A, Behnam H, Noroozian M, Mohammadi MR, Mohammadi M (2009) Abnormalities of quantitative electroencephalography in children with Asperger disorder in various conditions. *Research in Autism Spectrum Disorders* **3(2)**, 538-546.

[11] Filipek PA, Accardo PJ, Ashwal S, Baranek GT, Jr CE, Dawson G, Gordon B, Gravel JS, Johnson CP, Kallen RJ, Levy SE, Minshew NJ, Ozonoff S, Prizant BM, Rapin I, Rogers SJ, Stone WL, Teplin SW, Tuchman RF, Volkmar FR (2000) Practice parameter: screening and diagnosis of autism: report of the Quality Standards Subcommittee of the American Academy of Neurology and the Child Neurology Society. *Neurology* **55(4)**, 468-479.

[12] Sp VDB, Reinders F, Donderwinkel M, Peters MJ (1998) Volume conduction effects in EEG and MEG. *Electroencephalography and Clinical Neurophysiology* **106(6)**, 522-534.

[13] Coben R, Clarke AR, Hudspeth W, Barry RJ (2008) EEG power and coherence in autistic spectrum disorder. *Clinical Neurophysiology* **119(5)**, 1002-1009.

[14] Sheikhani A, Behnam H, Mohammadi MR, Noroozian M (2007) Analysis of EEG background activity in Autism disease patients with bispectrum and STFT measure. In, Proceedings of the 11th WSEAS International Conference on Communications (pp. 318-322).

[15] Sheikhani A, Behnam H, Mohammadi MR, Noroozian M (2007) Analysis of quantitative Electroencephalogram background activity in Autism disease patients with Lempel-Ziv complexity and Short Time Fourier Transform measure. In, Ieee/embs International Summer School and Symposium on Medical Devices and Biosensors (pp. 19-22).

[16] Sheikhani A, Behnam H, Mohammadi MR, Noroozian M, Golabi P (2008) Connectivity Analysis of Quantitative Electroencephalogram Background Activity in Autism Disorders with Short Time Fourier Transform and Coherence Values. In, international Congress on Image and Signal Processing (pp. 207-212).

[17] Rashidi M, Behnam H, Sheikhani A, Norouzian M, Rashidi M, Norouzian M (2010) Evaluation of EEG signal in autism disorder with ICA analysis. *Iranian Journal of Biomedical Engineering* **4(3)**, 187-194.

[18] Von Stein A, Sarnthein J (2000) Different frequencies for different scales of cortical integration: from local gamma to long range alpha/theta synchronization. *International Journal of Psychophysiology* **38(3)**, 301-313.

[19] Orekhova EV, Stroganova TA, Nygren G, Tsetlin MM, Posikera IN, Gillberg C, Elam M (2007) Excess of high frequency electroencephalogram oscillations in boys with autism. *Biological Psychiatry* **62(9)**, 1022-1029.

[20] Dumas G, Soussignan R, Hugueville L, Martinerie J, Nadel J (2014) Revisiting mu suppression in autism spectrum disorder. *Brain Research* **1585**, 108-119.

[21] Just MA, Keller TA, Malave VL, Kana RK, Varma S (2012) Autism as a neural systems disorder: a theory of frontal-posterior underconnectivity. *Neuroscience & Biobehavioral Reviews* **36(4)**, 1292-1313.

[22] Cohen IL (1994) An artificial neural network analogue of learning in autism. *Biological Psychiatry***36(1)**, 5-20.

[23] Gustafsson L (1997) Inadequate cortical feature maps: a neural circuit theory of autism. *Biological Psychiatry* **42(12)**, 1138-1147.

[24] Mcclelland JL (2000) The basis of hyperspecificity in autism: a preliminary suggestion based on properties of neural nets. *Journal of Autism & Developmental Disorders* **30(5)**, 497-502.

[25] O'Loughlin C, Thagard P (2000) Autism and coherence: A computational model. *Mind & Language* **15(4)**, 375-392.

[26] Brock J, Brown CC, Boucher J, Rippon G (2002) The temporal binding deficit hypothesis of autism. *Development & Psychopathology* **14(2)**, 209-224.

[27] Niederhoefer C, Gollas F, Tetzlaff R (2006) EEG analysis by multi layer Cellular Nonlinear Networks (CNN). In, IEEE Biomedical Circuits and Systems Conference (pp. 25-28).

[28] Niederhofer C, Gollas F, Tetzlaff R (2008) Dynamics of EEG-signals in epilepsy: Spatio temporal analysis by Cellular Nonlinear Networks. In, 18th European Conference on Circuit Theory and Design (pp. 296-299).

[29] Niederhofer C, Tetzlaff R (2005) Recent results on the prediction of EEG signals in epilepsy by discrete-time cellular neural networks (DTCNN). *IEEE International Symposium on Circuits and Systems* **32(1)**, 5218-5221.

[30] Müller J, Müller J, Tetzlaff R (2011) A new cellular nonlinear network emulation on FPGA for EEG signal processing in epilepsy. In, Bioelectronics, Biomedical, and Bioinspired Systems V; and Nanotechnology V **8068**, 80680M.

[31] Bjürne P, Balkenius C (2005) A model of attentional impairments in autism: first steps toward a computational theory. *Cognitive Systems Research* **6(2)**, 193-204.

[32] Grossberg S, Seidman D (2006) Neural dynamics of autistic behaviors: cognitive, emotional, and timing substrates. *Psychological Review* **113(3)**, 483-525.

[33] Noriega G (2007) Self-organizing maps as a model of brain mechanisms potentially linked to autism. *IEEE Transactions on Neural Systems & Rehabilitation Engineering* **15(2)**, 217-226.

[34] Noriega G (2015) A neural model to study sensory abnormalities and multisensory effects in autism. *IEEE Transactions on Neural Systems & Rehabilitation Engineering* **23(2)**, 199-209.

[35] Papageorgiou EI, Kannappan A (2012) Fuzzy cognitive map ensemble learning paradigm to solve classification problems: Application to autism identification. *Applied Soft Computing Journal* **12(12)**, 3798-3809.

[36] Association AP (2013) *Diagnostic and statistical manual of mental disorders (DSM-5®)*. Washington, D.C., American Psychiatric Pub.

[37] Woolger C (2001) Wechsler intelligence scale for children-(WISC-III). In, Dorfman WI and Hersen M (eds.)*Understanding Psychological Assessment* (pp. 219-233). Boston, Springer.

[38] Liu Y, Jiang X, Cao T, Wan F, Peng UM, Mak PI, Vai MI (2012) Implementation of SSVEP based BCI with Emotiv EPOC. In, IEEE International Conference on Virtual Environments Human-Computer Interfaces and Measurement Systems (pp. 34-37).

[39] Liu Y, Zhou W, Yuan Q, Chen S (2012) Automatic seizure detection using wavelet transform and SVM in long-term intracranial EEG. *IEEE Transactions on Neural Systems & Rehabilitation Engineering* **20(6)**, 749-755.

[40] Chua LO, Roska T (1993) The CNN paradigm. *IEEE Transactions on Circuits systems I, Fundamental Theory applications* **40(3)**, 147-156.

[41] Nunez PL, Srinivasan R (2006) *Electric fields of the brain: the neurophysics of EEG*. Oxford, Oxford University Press.

[42] Mohammadi Z, Frounchi J, Amiri M (2017) Wavelet-based emotion recognition system using EEG signal. *Neural Computing & Applications* **28(8)**, 1985-1990.

[43] Arnau-González P, Arevalillo-Herráez M, Ramzan N (2017) Fusing highly dimensional energy and connectivity features to identify affective states from EEG signals. *Neurocomputing* **244**, 81-89.

[44] Das AB, Bhuiyan MIH (2016) Discrimination and classification of focal and non-focal EEG signals using entropy-based features in the EMD-DWT domain. *Biomedical Signal Processing & Control* **29**, 11-21.

[45] Gandhi TK, Panigrahi BK, Anand S (2011) A comparative study of wavelet families for EEG signal classification. *Neurocomputing* **74(17)**, 3051-3057.

[46] Dhiman R, Saini JS, Priyanka (2017) Biogeography Based Hybrid Scheme for Automatic Detection of Epileptic Seizures from EEG Signatures. *Applied Soft Computing* **51**, 116-129.

[47] Ban JC, Chang CH (2016) When are two multi-layer cellular neural networks the same? *Neural Networks* **79(C)**, 12-19.

[48] Gilli M, Roska T, Chua LO, Civalleri PP (2002) CNN dynamics represents a broader class than PDEs. *International Journal of Bifurcation & Chaos* **12(10)**, 2051-2068.

[49] Chua LO, Yang L (1988) Cellular neural networks: theory. *IEEE Transactions on Circuits & Systems* **35(10)**, 1257-1272.

[50] Behnam H, Sheikhani A, Mohammadi MR, Noroozian M, Golabi P (2008) Abnormalities in Connectivity of Quantitative Electroencephalogram Background Activity in Asperger Disorders with Short Time Fourier Transform and Coherence Values. *in: Proceedings of Tenth International Conference on Computer Modeling and Simulation* **40(3)**, 76-81.

[51] Sheikhani A, Behnam H, Mohammadi MR, Noroozian M, Mohammadi M (2012) Detection of abnormalities for diagnosing of children with autism disorders using of quantitative electroencephalography analysis. *Journal of Medical Systems* **36(2)**, 957-963.

[52] Barttfeld P, Wicker B, Cukier S, Navarta S, Lew S, Sigman M (2011) A big-world network in ASD: dynamical connectivity analysis reflects a deficit in long-range connections and an excess of short-range connections. *Neuropsychologia* **49(2)**, 254-263.